1990

The Scroll Compressor with Variable Capacity Control Mechanism for Automotive Air Conditioner

T. Hirano
Mitsubishi Heavy Industries

T. Shipoka
Mitsubishi Heavy Industries

THE SCROLL COMPRESSOR WITH VARIABLE CAPACITY CONTROL MECHANISM FOR AUTOMOTIVE AIR CONDITIONER

TAKAHISA HIRANO

TETSUO SHIGEOKA

Nagoya Research & Development Center
Mitsubishi Heavy Industries, Ltd., Nagoya, Japan

ABSTRACT

We have developed the scroll compressor with variable capacity control mechanism. The amount of bypassed gas from the compression chamber to the suction chamber is controlled by displacement of the bypass piston.

This paper presents as follows.

The analytical technique for calculating performance of the compressor with by-pass-type capacity control mechanism has been developed.

Also, experimental loss analysis by measurement of P-V diagram has been carried out. The result of calculating performance has good agreement with that of experimental loss analysis.

INTRODUCTION

Recently, the compressor with variable capacity control mechanism for automotive air conditioners has been remarkably developed to satisfy the following requirements.

(1) to keep the automotive cabin temperature comfortable

(2) to improve driving feeling

(3) to drive the system economically through all seasons

We have developed the scroll compressor with excellent quality as that for automotive airconditioners[1)-5)], and a by-pass-type mechanism is adopted as the continuous capacity control. The capacity control mechanism, which changes the channel area of the bypass hole continuously according to the suction gas pressure, has been developed. The development of performance simulation program, the measuring results of internal behavior and the results of loss analysis for capacity control compressor are described below.

STRUCTURE AND PRINCIPLES

Fig.1 shows the cross sectional view of the scroll compressor for automotive air conditioners.

Main components for capacity control are as follows.

(1) Fixed scroll provided with the bypass holes at 50% displacement and the discharge port.

(2) Sliding bypass piston in the fixed scroll.

(3) Pressure generating valve fixed to the housing.

Fig.2 shows a cross sectional view of the pressure generating valve which generates the control pressure Pa regulating the displacement of the bypass piston.

Fig.3 is V-θ diagram (V: the cylinder volume, θ: the rotation angle) representing the position of the bypass hole. The capacity control in range of 100 to 50% becomes available by changing suitably the opening area of the bypass hole provided at the portion of 50% displacement, while the capacity from 50 to 0% can be controlled by the bypass hole provided within the discharge port (position of 0% displacement). As result continuous capacity control from 100 to 0% can be achieved by these bypass holes.

Fig.4 illustrates operation principal of the capacity control mechanism. Both the discharge gas pressure P_H and the suction gas pressure P_L are higher under the environmental conditions when cooling load is higer. In this case the bellows is contracted by the suction pressure and the three-way valve is opened. Then the control pressure P_a becomes higher. The bypass piston moves to the left to close the bypass holes leading to the operation at max. capacity. When operated under the environmental conditions of lower cooling load, both the discharge pressure P_H and the suction pressure P_L become lower. Then the three-way valve is closed and the control pressure becomes lower. The bypass piston is moved to the right to open the bypass hole by the spring force and the pressure difference ($P_a - P_L$) leading to the operation at controlled capacity.

PERFORMANCE ANALYSIS UNDER CONTROLLED CAPACITY

For predicting the cylinder pressure, the power consumption and the capacity under controlled capacity, the performance simulation program has been developed.

Assumption

(1) It is assumed that the cylinder pressure over entire strokes from suction to discharge is polytropic process.

(2) The cylinder volume change to the rotation angle θ is based on the volume change curve of P.M.P. (Perfect Meshing Profile)*.

(3) The flow rate from the bypass hole is given by the equation of nozzle flow.

(4) There is no leakage except at the bypass hole.

Analytical model

Fig.5 shows the analytical flow chart to give the capacity control rate and the indicated efficiency. The cylinder pressure and the outflow rate of refrigerant from the bypass hole can be given by the following equations.

1. The cylinder pressure

$$P(\theta) = P_L \left(\frac{V_L}{V(\theta)} \right)^n \quad \cdots\cdots\cdots \quad (1)$$

Where P_L : Suction gas pressure

V_L : Suction chamber volume

n : Polytropic index

P : Cylinder pressure

$V(\theta)$: Cylinder volume

Where the cylinder volume change is given as follows.

$$V(\theta) = \pi b \rho \left(2\theta + \frac{\rho}{b} + \pi\right) L \quad \cdots\cdots\cdots \quad (2)$$

Where θ : Rotation angle

b : Radius of involute base circle

ρ : Orbiting radius

L : Height of scroll

2. The cylinder pressure at bypass process and the outflow rate of refrigerant from the bypass hole.

(1) Equation of State

$$\frac{dP}{dt} = nP \left(-\frac{1}{V}\frac{dV}{d\theta} + \frac{1}{W}\frac{dW}{d\theta} \right) \quad \cdots\cdots\cdots \quad (3)$$

where W : Gas amount in the cylinder

V : Cylinder volume

(2) Equation of continuity

$$\frac{dW}{d\theta} = -\frac{G}{\omega} \quad \cdots\cdots \quad (4)$$

where G : Outflow rate to the suction chamber from the bypass hole

ω : Rotational speed

(3) Equation of flow

The outflow rate of refrigerant gas to the suction chamber from the by-bass hole is given as follows.

$$G = \begin{cases} CA\sqrt{\dfrac{2\kappa g}{\kappa-1}\cdot\dfrac{P}{v}\left\{\left(\dfrac{P_L}{P}\right)^{2/\kappa}-\left(\dfrac{P_L}{P}\right)^{(\kappa+1)/\kappa}\right\}} & \text{at } \left(\dfrac{2}{\kappa+1}\right)^{\kappa/(\kappa-1)} \leqq \dfrac{P_L}{P} \leqq 1 \\ CA\sqrt{\kappa g\dfrac{P}{v}\cdot\left(\dfrac{2}{\kappa+1}\right)^{(\kappa+1)/(\kappa-1)}} & \text{at } 0 \leqq \dfrac{P_L}{P} \leqq \left(\dfrac{2}{\kappa+1}\right)^{\kappa/(\kappa-1)} \end{cases} \quad \cdots\cdots \quad (5)$$

where κ : Ratio of specific heats of refrigerant gas

g : Acceleration of gravity

v : Specific volume of refrigerant gas in the cylinder

C : Coefficient of the flow rate of the bypass hole

A : Channel area of the bypass hole

(4) Opening area of the bypass hole

The opening area of the bypass hole is defined by the rotation angle and the characteristics of the bypass piston, and given by the equation shown below.

$$A = C_A(P_L, P_a)Av(\theta) \quad \cdots\cdots \quad (6)$$

where $C_A(P_L, P_a)$: Throttling rate of the bypass channel area

Av : Bypass channel

In addition the following relation is found between P_L and P_a.

$$P_a = aP_L + bP_H + C \quad \cdots\cdots \quad (7)$$

where P_H : Discharge pressure

a, b, c : Constants to define characterstics of the pressure generating valve.

(5) Theoretical gas compression work

The theoretical gas compression work is the compression power given when the suction gas presents adiabatic change, while the displacement of the compressor is required in order to provide it. However, in case of the capacity control mechanism which requires continuous change in the channel area of the bypass hole, the displacement of the compressor can not be equally determined. Thus in this paper the equivalent displacement Veq. is given by the amount of the discharge assuming the volumetric efficiency is 100%, by which the theoretical gas compression work Weq. is computed.

$$Weq. = \frac{1}{\kappa - 1} P_L \cdot Veq \left\{ \left(\frac{P_H}{P_L} \right)^{\frac{\kappa - 1}{\kappa}} - 1 \right\} \quad \ldots\ldots\ (8)$$

When the equations (3), (4) and (5) are solved simultaneously, the cylinder pressure and the gas amount in the cylinder under controlled capacty are given. This is a matter of initial value with regard to unknown values, the pressure and the gas amount and solved by the Runge -Kutta method numerically.

P-V diagram given by this simulation is shown in Fig. 6. The diagram shows the cylinder pressure for change in the opening area of the bypass holes.

MEASURING RESULTS OF INTERNAL BEHAVIOR

Pressure in the cylinder

Six pressure sensors were set in total, of which are three at the outer side of scroll, two at the inner side of scroll of the fixed scroll, and one at the discharge port.

Two gap sensors were positioned for measuring the position of the bypass piston and the displacement of the discharge valve.

Fig.7 shows P-θ diagram measured at 67% capacity.

P-V diagram when the capacity control rate is changed.

Fig.8 shows P-V diagram given under the bypass piston controlled at different positions. In this range only 50% bypass hole shows operation under opening state. As the capacity control rate increases, the cylinder pressure decreases in the opening range of 50% bypass hole.

The pressure rising is almost nil from the end of suction process to the position of 50% displacement as shown in Fig. 8 (B - curve), which is ideal state. In case of A - curve when 50% bypass hole is partially open, the cylinder pressure rises smoothly after the end of suction process in the proportional capacity zone. The behavior became clear in the method for the continuous capacity control by changing the opening area of the by-pass hole continuously.

Influence of compressor speed

Fig.9 shows P-V diagram given when the compressor speed is changed with the same opening area of 50% bypass hole. As the compressor speed increases, P-V diagram expands as a whole.
This is due to decrease the opening time of the bypass hole caused by increasing the compressor speed.

Influence of suction gas state

Fig. 10 shows P-V diagram under 0.83 dryness fraction and 18 degrees of superheat of the suction gas with the same opening area of 50% bypass hole. A slightly contracted pattern is shown in P-V diagram under 0.83 dryness fraction, but the actual power consumption for the compressor indicates a little larger value than that under the superheated vapour. In loss analysis when operated under the wet vapour, it is required to take the effect of latent heat of vapourization into consideration.

Analysis of loss

Fig. 11 shows the results of loss analysis provided by the measuring results of the cyliner pressure when the stroke of the bypass piston is changed at N=2000 min^{-1}. The mechanical efficiency constants to the wide change in the capacity control rate. This value is reduced about 5% when the compressor speed is set to 4000 min^{-1}. As the capacity control rate increases, the discharge loss decreases about 2.4% in the range of 100 to 30% capacity. The indicated efficiency decreases significantly as the capacity control rate increases. This is due to compression loss caused by connection of the compression chamber at the inner central portion and two symmetrical compression chambers at next outer side and also due to the higher flow resistance of the bypass hole. This tendency applies to the zone where compressor speed is higher.

The loss of endothermic amount caused by wet refrigerant should be taken into account in loss analysis at operation under wet vapour. The compression heat is absorbed by the latent heat of liquid refrigerant in the actual wet vapour compression, which results in change of pressure in accordance with lower polytropic index rather than by the gas under superheated state. The power consumption for this endothermic amount can not be analyzed from the P-V diagram. Thus the loss is assumed to be included in the indicated loss, and the mechanical efficiency is supposed not to change in the suction gas state in this paper. The results under such state is shown in Fig. 12.

COMPARISON OF ANALYTICAL RESULTS WITH EXPERIMENTAL RESULTS

Fig. 13 shows the results of calculating performance and the results of loss analysis given by the meaurement under capacity control. The indicated power consumpstion shows good agreement over wide range. Circulating amount of refrigerant is larger in relative error when the capacity control rate is higher. The reason is interpreted that the heat balance of bypass gas and suction gas under controlled capacity is not taken into account in this paper.

CONCLUSION

The following is concluded with that we have conducted performance simulation and detailed measurement of internal behavior of the compressor under controlled capacity.

(1) In the scroll compressor with bypass type capacity control mechanism the pressure in the cylinder, behavior of the bypass piston under controlled capacity and the influence of capacity control rate, compressor speed and the state of suction gas over such items were clarified. As the results, many elements of knowledge in design were understood with regard to bypass-type capacity control.

(2) The performance simulation has been developed regarding the bypass holes as nozzle flow and the effectiveness was verified, which will be utilized in future activities.

REFERENCES

1) Hirano et al., Proc. of the 1988 Int. Comp. Conf. at Purdue Vol. 1, P.65
2) Hirano et al., Mitsubishi Heavy Industries Technical Review, Vol. 26. No. 1, 1989-1, P. 66
3) Hagimoto et al., Mitsubishi Heavy Industries Technical Review, Vol. 23, No.2., 1986-3, P.154
4) Hagimoto et al., Proc. of the 20th Japanese Joint Conf. on Air Conditioning & Refrigeration, 1986-4, P117.
5) Asanabe et al., Mitsubishi Heavy Industries Technical Review, Vol. 23, No.2, 1986-3, P-171
6) Patent Application No. 62-017074, Patent Application No.62-166450 and others.

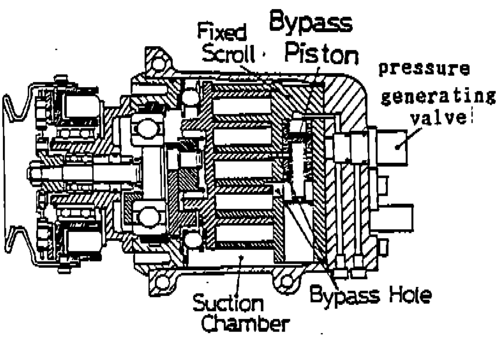

Fig 1. Cross sectional view of Scroll compressor

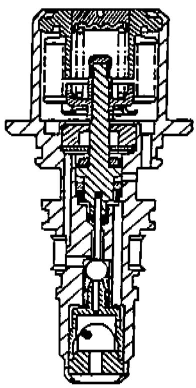

Fig 2. Cross sectional view of pressure generating valve

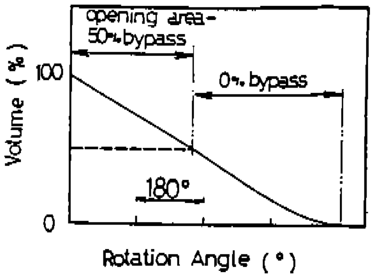

Fig 3. Position of the bypass ports

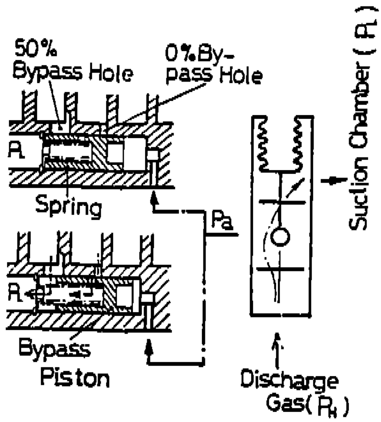

Fig 4. Principle of Capacity control

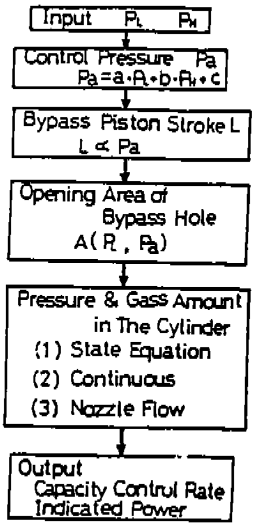

Fig 5. Analytical flow chart

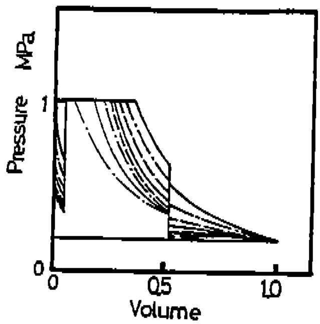

Fig 6. Analytical result

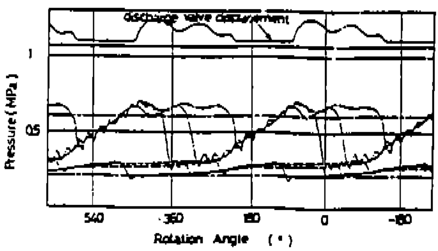

Fig 7. Experimental result of pressure in the cylinder

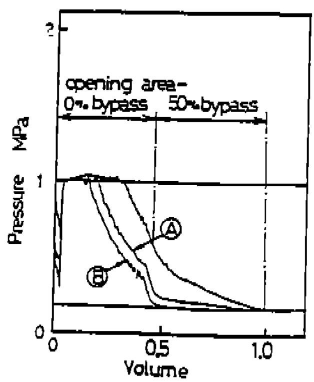

Fig 8. Variation of PV diagram with control rate of capacity

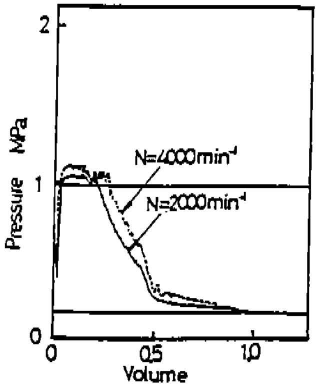

Fig 9. Variation of PV diagram with compressor speed

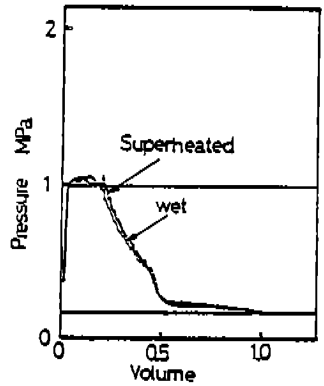

Fig10. Variation of PV diagram with suction gas state

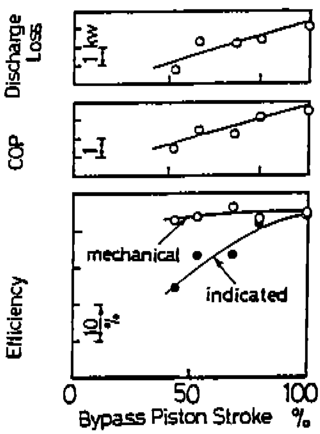

Fig11. Analysis of loss in capacity controled

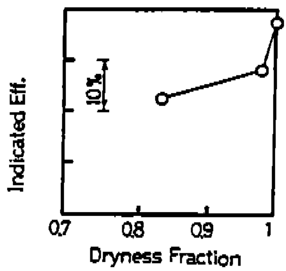

Fig12. Variation of adiabatic efficiency with dryness fraction of suction gas

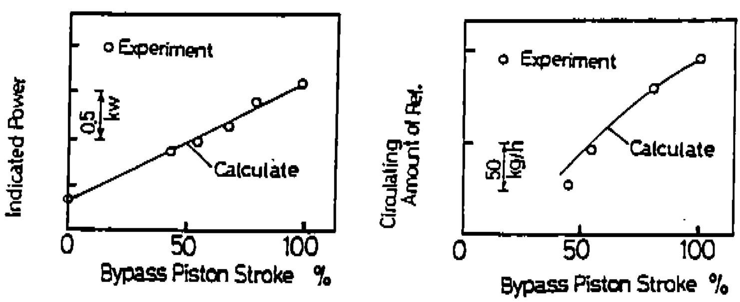

Fig13. Comparison of analytical results with experimental results